

## Video Article

# In Situ Lithiated Reference Electrode: Four Electrode Design for In-operando Impedance Spectroscopy

Kaushik Kalaga<sup>1</sup>, Marco-Tulio F. Rodrigues<sup>1</sup>, Daniel P. Abraham<sup>1</sup>
<sup>1</sup>Chemical Sciences and Engineering Division, Argonne National Laboratory

Correspondence to: Kaushik Kalaga at [kkalaga@anl.gov](mailto:kkalaga@anl.gov)

URL: <https://www.jove.com/video/57375>

DOI: [doi:10.3791/57375](https://doi.org/10.3791/57375)

Keywords: Chemistry, Issue 139, Electrochemical Impedance Spectroscopy, 4-electrode cell, Reference Electrode, Lithium ion battery, Diagnostic protocol, In-operando

Date Published: 9/12/2018

Citation: Kalaga, K., Rodrigues, M.T., Abraham, D.P. In Situ Lithiated Reference Electrode: Four Electrode Design for In-operando Impedance Spectroscopy. *J. Vis. Exp.* (139), e57375, doi:10.3791/57375 (2018).

## Abstract

Extending operating voltage of Li-ion batteries results in higher energy output from these devices. High voltages, however, may trigger or accelerate multiple processes responsible for long-term performance decay. Given the complexity of physical processes occurring inside the cell, it is often challenging to achieve a full understanding of the root causes of this performance degradation. This difficulty arises in part from the fact that any electrochemical measurement of a battery will return the combined contributions of all components in the cell. Incorporation of a reference electrode can solve part of the problem, as it allows the electrochemical reactions of the cathode and the anode to be individually probed. A variation in the voltage range experienced by the cathode, for example, can indicate alterations in the pool of cyclable lithium ions in the full-cell. The structural evolution of the many interphases existing in the battery can also be monitored, by measuring the contributions of each electrode to the overall cell impedance. Such wealth of information amplifies the reach of diagnostic analysis in Li-ion batteries and provides valuable input to the optimization of individual cell components. In this work, we introduce the design of a test cell able to accommodate multiple reference electrodes, and present reference electrodes that are appropriate for each specific type of measurement, detailing the assembly process in order to maximize the accuracy of the experimental results.

## Video Link

The video component of this article can be found at <https://www.jove.com/video/57375/>

## Introduction

The demand for high energy densities from Li-ion batteries (LIBs) is driving research towards understanding fundamental factors that limit Li-ion cell performance<sup>1</sup>. High voltage operation of cells containing a new generation of layered transition metal oxide cathodes, graphite anodes and organic carbonate electrolytes is associated with several parasitic reactions<sup>2,3</sup>. Some of these reactions consume Li-ion inventory and often result in significant impedance rise of the cell<sup>4,5,6,7</sup>. Loss of Li-ion also results in a net shift of the surface potentials of electrodes. Monitoring of voltage changes on an individual electrode in a full cell versus a reference electrode (RE) can be performed in commercial 3-electrode cell designs<sup>8,9,10,11,12,13,14</sup>. Information pertaining to voltage profiles and the impedance changes on individual electrodes promotes a deeper understanding of the fundamental degradation mechanisms of a LIB. Conventional 3-electrode cells contain Li metal as a reference electrode, which facilitates a distinct understanding of the electrochemical processes at each electrode. Li-metal in contact with the organic electrolyte undergoes spontaneous surface modification and the contribution of this surface layer on Li cannot be quantified<sup>15</sup>. Several 3-electrode configurations such as (a) T-model, (b) a micro-RE positioned coaxial to both the working and the counter electrode, (c) a coin cell with an RE at the back of the counter electrode, etc. have been proposed earlier. Most of these cell configurations have the RE positioned away from the cell sandwich, generating significant drift in the impedance data due to low conductivity of the electrolyte. It has been proven that a RE with a stable potential throughout the measurement must be stationed in the center of the sandwich to ensure reliable impedance data.

In order to address these discrepancies, we have designed a cell setup involving a fourth RE<sup>16</sup>. An ultra-thin Sn plated Cu wire is sandwiched in between the electrodes of a battery that can be electrochemically lithiated *in situ* to form a Li<sub>x</sub>Sn alloy. As Sn undergoes lithiation, the voltage of the reference wire drops and a completely lithiated wire has a potential close to 0 V vs. Li<sup>+</sup>/Li<sup>0</sup><sup>17</sup>. The lithiated composition has a potential comparable to Li metal and the metastable alloys facilitate a stable potential during the time period of the measurement. A Li metal exposed to the electrolyte is prone to electrolyte decomposition products forming surface layers. An EIS measurement to probe the impedance of individual electrodes by collecting spectra between one of the electrodes and the Li metal reference as coupled have not been reliable due to the contribution of these layers on the impedance. Although electrolyte reduction is inevitable also on the Li-Sn surface, an *in situ* lithiated reference wire has the following advantages: (a) no constant electrolyte decomposition products as the voltage is always above the decomposition potential of the electrolyte unless lithiated, implying no loss of Li inventory in the system to interfacial layers; (b) layers formed during lithiation of the Sn wire are over a very small area, providing negligible contribution to the EIS data; and (c) the formed products degrade as the Sn wire loses Li and the potential of the wire increases, resulting in lithiation of fresh Sn wire during every lithiation and thus formation of very thin interfacial layers every time instead of increased thickness of these layers. Spectra recorded with these alloys as reference provide more accurate and reliable data of the electrode impedance. We conducted tests with standard 2032-type coin cells and 4-electrode

RE cells to validate our design. Results from these tests and our interpretation of the data will be used as a representative result to explain the efficacy of our protocol. The 3–4.4 V cycling followed a standard protocol, which included formation cycles, aging cycles, and periodic AC impedance measurements during the cycling. The coin cell measurements provide valuable information on the parameters such as cycle life, capacity retention, AC impedance changes, etc. RE cells enable monitoring voltage changes and impedance rise on individual electrodes. Our mechanistic understanding into the capacity fade and impedance rise can provide guidelines for the development of electrolyte systems and understand contributions for capacity loss from each electrode during high-voltage cell operation.

Our cells contained  $\text{Li}_{1.03}(\text{Ni}_{0.5}\text{Co}_{0.2}\text{Mn}_{0.3})_{0.97}\text{O}_2$  (denoted here as NMC532)-based positive electrodes, graphite-based negative electrodes (denoted here as Gr) and a 1.2 M solution of  $\text{LiPF}_6$  in Fluoroethylene Carbonate (FEC):Ethyl Methyl Carbonate (EMC) (5:95 w/w) as the electrolyte. The electrodes used in this study are standard electrodes fabricated at the Cell Analysis, Modeling and Prototyping (CAMP) Facility at Argonne National Laboratory. The positive electrode consists of NMC532, conductive carbon additive (C-45) and polyvinylidene fluoride (PVdF) binder in a weight ratio of 90:5:5 on a 20  $\mu\text{m}$  thick Al current collector. The negative electrode consists of graphite, mixed with C-45, and PVdF binder in a weight ratio of 92:2:6 on a 10  $\mu\text{m}$  thick Cu current collector. Circular discs of 5.08 cm diameter were punched from the electrode laminates and the separators were punched with a 7.62 cm die for use in fixtures with 7.62 cm inner diameter. These electrodes were dried at 120 °C and the separators at 75 °C in a vacuum oven for at least 12 h prior to the cell assembly. A schematic representation of the fixture design is represented in **Figure 1**. Large fixtures and electrodes ensure minimum inhomogeneities in current distributions per unit area, thus, providing the least distortions in the impedance spectra. The 3–4.4 V cycling followed a standard protocol, which included two formation cycles at a C/20 rate, 100 ageing cycles at a C/3 rate and two diagnostic cycles at C/20. All battery tests were conducted at 30 °C. Electrochemical cycling data was measured using a battery cycler and the electrochemical impedance spectroscopy (EIS) is performed using a potentiostat system.

## Protocol

### 1. Stripping Copper/Tin Wires

- Heat commercially obtained stripping solution.
  - Pour commercial industrial grade stripping solution into a stainless steel beaker (7.6 cm in diameter and 8.5 cm in height) to a depth of about 5 mm from the bottom. Place the beaker on to a hot plate. Begin heating a slow rate of about 5 °C/min.
  - Immerse a portable thermocouple into the solution to closely monitor the temperature ramp of the solution and adjust the heating rate of the hot plate to maintain at the required heating rate.
- Setting up of the Cu/Sn wire on the jig for preparing reference wires.
  - Wind a thick copper wire in the form of a jig (4 cm wide and 7 cm long). Mount the commercial Cu/Sn (or pure Cu) wire (25.4  $\mu\text{m}$  in diameter), plated with a thin layer of Sn and electronically insulated with a polyurethane coating) onto the jig as shown in **Figure 1a**. NOTE: These wires are extremely delicate and may break if handled rough.
- Stripping the polymer
  - Once the temperature of the stripping solution reads about 85 °C on the thermocouple, stop heating the solution and immerse the wire mounted jig into the solution.
  - Leave the jig inside the solution for 15 s and then rinse the jig in DI water for another 15 s to wash excess stripping solution adsorbed onto the wire.
  - Check the wire for exposed Sn (appears as silvery white color) and repeat step 1.3.2 until the polymer is completely stripped. **CAUTION:** Long term exposure of the wire to the stripping solution can etch away Sn coating and expose a reddish-brown Cu wire underneath. If the wires are being prepared for impedance spectroscopy analysis, the presence of Sn plating is essential.
  - Rinse the jig in DI water and dry in air at room temperature (25 °C).
  - Cut the wires in the middle of the stripped regions to obtain wires with both ends with exposed Sn (or Cu over excess stripped wires). The size of each wire is approximately 10 cm.

### 2. Reference Wire Preparation

- To make the reference wire contacts, connect the wires to an electrical wire and solder the junction.
  - From a roll of electrical circuit wires, cut pieces of 10 cm and strip the insulation cover from both the ends to expose about 2 cm of metal.
  - Mount one end of the polymer stripped wire on to the end of the exposed electrical wire and solder the junction to form an electrical contact between the wires.
  - Measure the resistance between the exposed Sn (or Cu) wire and the exposed electrical wire. NOTE: The typical resistance values are between 6–8  $\Omega$ .
  - Transfer one wire each with Sn exposed and with Cu exposed into an Argon filled glovebox for assembly into a cell.
- Mount a pressed and flattened Li metal foil to the Cu exposed reference wire
  - Cut a small piece of Li metal (not more than 5 mm x 5 mm) from a large Li foil inside the glovebox. NOTE: Use dedicated equipment for contact with Li metal and store inside the glovebox to prevent cross contamination and subsequent electrical micro-short.
  - Using a roller covered with a polymer tape (to prevent sticking of the Li metal onto the metallic roller surface), roll the Li metal piece on a Teflon platform under Ar.
  - Continue rolling to achieve a foil thickness of approximately 25  $\mu\text{m}$ . Check the thickness using a screw gauge.
  - Upon obtaining the desired thickness of the Li metal foil, bend the foil at the center to form a U- shape. Place the Cu exposed wire in between the bend such that Cu is in contact with the Li metal and press the fold to encapsulate Cu wire between the two Li layers.

NOTE: Maintain extreme caution while encapsulating Cu wire so as to ensure covering all of the exposed tip. Cu is for electronic conductance only and contact of Cu to the electrolyte will result in reading a mixed surface potential generating erroneous voltage values in the data.

### 3. Cell Assembly and Data Acquisition

1. Place both the Li metal reference and the Sn reference wires in between the Li-ion cell assembly.
  1. Place the negative electrode in the fixture such that the center of the electrode is slightly shifted from the center of the fixture. Add 400  $\mu\text{L}$  of the electrolyte (1.2M LiPF<sub>6</sub> in Fluoroethylene Carbonate (FEC):Ethyl Methyl Carbonate EMC (5:95 w/w)) to wet the entire electrode.
  2. Place one separator on top of the electrode and using a organophobic sweep, gently eliminate trapped air bubbles between the separator and the electrode. Adjust the placement of the separator to ensure concentricity with the fixture to completely insulate the base of the fixture from the positive electrode and avoid electric short inside the cell.  
NOTE: Large electrodes tend to trap air pockets between the separator and the electrodes as they curl upon addition of the electrolyte. These air pockets need to be removed to ensure proper contact of the separator with the electrodes. The air bubbles increase the impedance of the cell and inhibit ion transfer.
  3. Add two drops (about 10  $\mu\text{L}$ ) of electrolyte, one at 2 mm away from the cell sandwich and another one at the center of the electrode. Position the Sn exposed tip of the reference wire at the center of the electrode and the Li metal foil (encapsulated onto Cu wire) on the drop away from the electrode. The surface tension between the metals and the electrolyte drops hold the wires in position.
  4. Add one more drop (about 10  $\mu\text{L}$ ) of electrolyte onto the Li metal after placing the wire in position.
  5. Remove additional air bubbles between the Li foil and the separator with the Teflon sweep. Add another 400  $\mu\text{L}$  of the electrolyte.
  6. Place a second separator aligned to the first separator such that both the reference wires are sandwiched between the two separators. Remove any additional air bubbles.  
**CAUTION:** While placing the second separator, excessive tension can break the reference wires. Leave extra wire inside the cell to reduce tension in the wire.
  7. Wet the positive electrode with 400  $\mu\text{L}$  of the electrolyte. Place the electrode aligned with the negative electrode on top of the second separator.
  8. Place the stainless steel spacer onto the positive electrode carefully to not disturb the cell stack alignment.  
NOTE: Misaligned electrodes result in inhomogeneous current distributions and reduced cell capacity due to reduced access of active cell area.
  9. Place two stainless steel wave springs on the puck to accommodate for cell volume changes and pressure build up which ensure proper electric contact between the electrodes and the fixture terminals. Close the fixture. Since the setup is not hermetically sealed, the tests are conducted inside the glove box in an inert atmosphere.
2. Record the data from the Li metal reference wire for individual electrode voltage profiles
  1. Connect the auxiliary reference terminal of the cycler to the Li metal while the positive and negative electrode terminals of the cycler are connected to the respective electrodes.  
NOTE: During the cycling of the cell, the cycler reads the potential difference between the positive terminal and the RE as Aux1 output and the negative electrode and the reference as Aux2. While the Li metal wire is connected, Aux1 and Aux2 are the potentials of individual electrodes with respect to Li metal.
3. Lithiate the Sn wire *in situ* to record electrochemical impedance spectroscopy (EIS).
  1. Apply a constant current of 5  $\mu\text{A}$  for 6 h between the positive electrode and the Sn wire with an upper voltage cutoff of 4 V to electrochemically lithiate the Sn. The potential of Li/Sn alloy thus formed is close to that of the Li metal. Disconnect the terminals and allow the wire to equilibrate for 2 h.  
NOTE: Ensure extremely low current (close to 0 A) in the circuit to confirm complete lithiation of the Sn wire.
  2. Alter cycler connections to Li metal to the auxiliary terminal of the cycler and Sn wire to the negative terminal of the cycler and ensure the reading of Aux2 close to 0 V. A lithiated phase of Sn is obtained, denoted as Li<sub>x</sub>Sn.
  3. Re-connect the positive and negative terminals of the cycler to the respective electrodes of the cell and the auxiliary terminal to Li<sub>x</sub>Sn wire.
4. Record EIS for (i) cathode vs. anode, (ii) cathode vs. lithiated Sn wire and (iii) anode vs. lithiated Sn wire. The impedance of (i) is the sum of the impedances obtained in (ii) and (iii). The potentiostat consists of two terminals to record the voltages and two for current outputs for each electrode.
  1. To obtain the full cell spectra, connect voltage and current terminals to the respective positive and negative electrodes of the cell.
  2. For the positive electrode impedance, connect the voltage and current positive terminals (also known as working electrode, WE) to the positive electrode, and connect the negative terminals (also known as the counter electrode, CE) to the Li<sub>x</sub>Sn reference electrode.
  3. For the negative electrode impedance, connect the WE terminals to the negative electrode and connect the CE terminals to the Li<sub>x</sub>Sn reference electrode.
  4. To record the EIS, supply AC currents or varying frequencies to cycle the electrochemical couple between a small voltage amplitude (5 mV) and plot the impedance response as imaginary component vs. the real component.

## Representative Results

**Figure 2** is a representative profile of the voltages of individual electrodes with 1.2M LiPF<sub>6</sub> in (FEC):EMC (5:95 w/w) as the electrolyte during the first and second cycles of formation. **Figure 3** shows the EIS spectra of the cell after three formation cycles and at the end of the cycle life ageing protocol. The ability to re-lithiate the RE to obtain EIS data aids in precise tracking of the impedance changes in individual electrode.

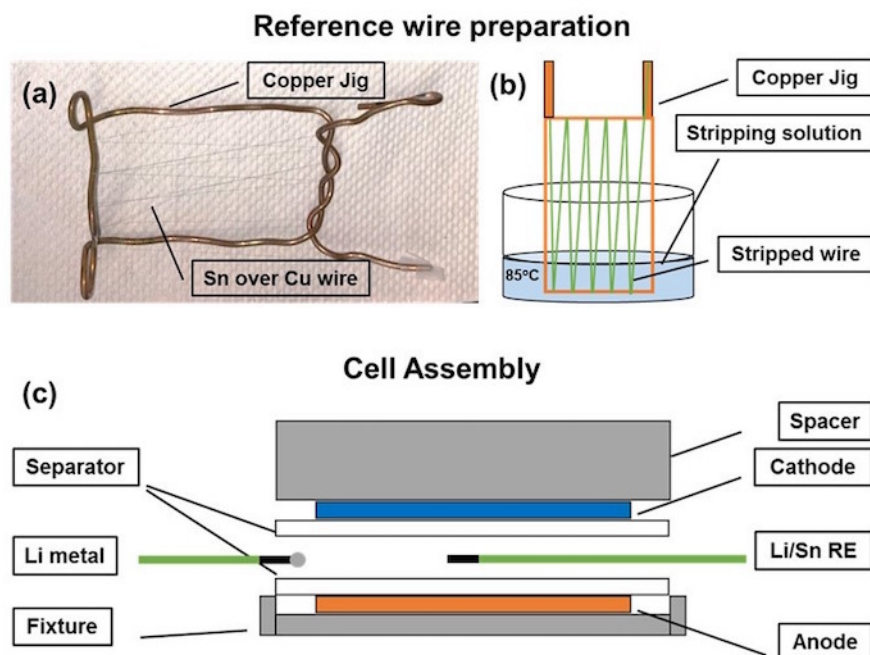


**Figure 1. Schematic and visual representation of the reference wire preparation and cell assembly**

(a) Copper jig used to mount the reference wires for stripping out the polymer coating, (b) A schematic of the stripping process indicating positioning of the jig inside the beaker to facilitate partial stripping of the wires to expose the Sn layer. The stripping solution is maintained at 85 °C. The jig is not completely immersed into the solution so that only a portion of the wire is stripped of the polymer layer. The wire is cut in the middle of the stripped part to create separate wires with exposed metal tips. (c) Schematic representation of the cell fixture design showing the position of both the reference electrodes. The cell contains both Li metal reference placed close to the cell stack and Li/Sn reference wires positioned in the center of the cell stack. [Please click here to view a larger version of this figure.](#)

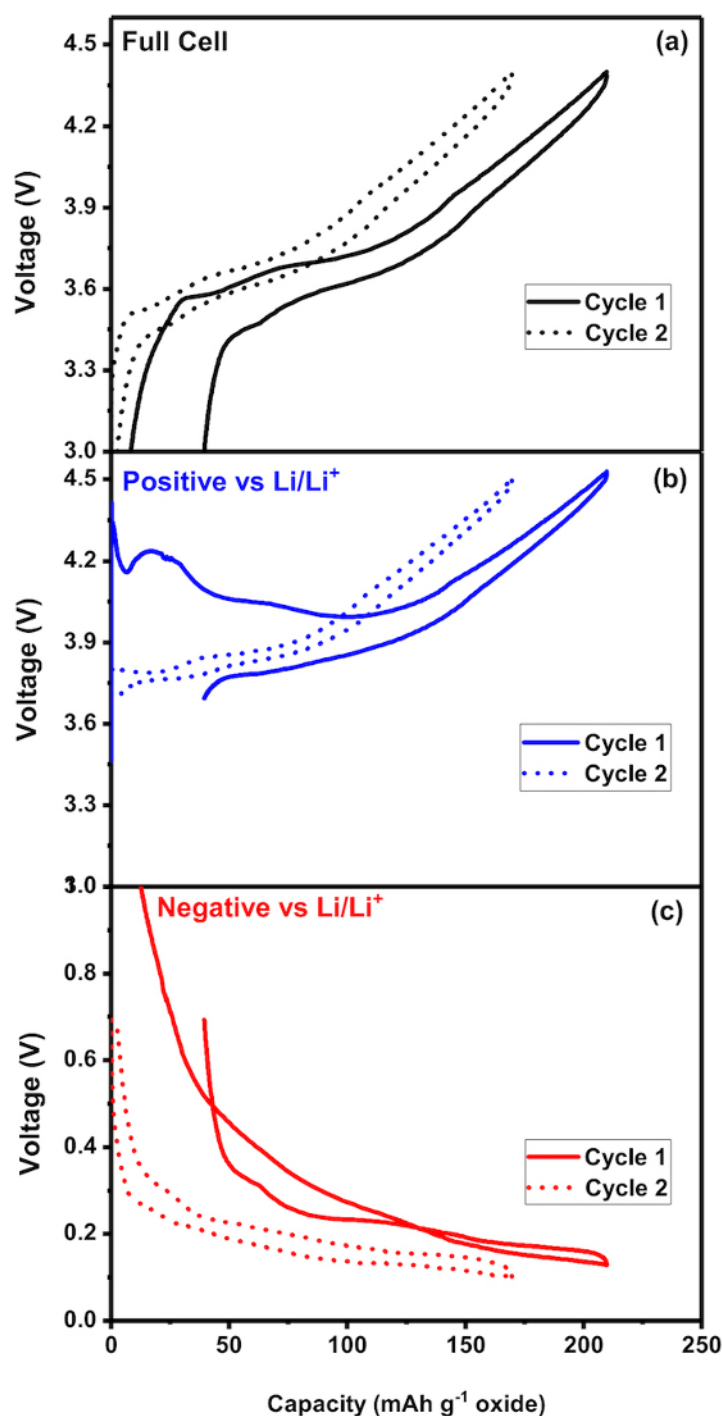


**Figure 2. Voltage profiles of the full cell, positive and negative electrodes**

(a) Voltage profile of the full cell in the first and second cycles between 3 and 4.4 V and the corresponding profiles of the positive and the negative electrodes vs Li/Li<sup>+</sup> is shown in (b) and (c) respectively. While the full cell sweeps between 3 and 4.3 V, the positive experiences voltages between 3.7 and 4.5 V. The negative undergoes voltage changes between 0.7 and 0.05 V. The Li reference wire enables close monitoring of individual electrodes and facilitates probing electrochemical redox reactions on the surface on individual electrodes. The plateau in each profile indicates precisely the voltage (vs Li/ Li<sup>+</sup>) at which lithiation/ de- lithiation occurs in an electrode. [Please click here to view a larger version of this figure.](#)

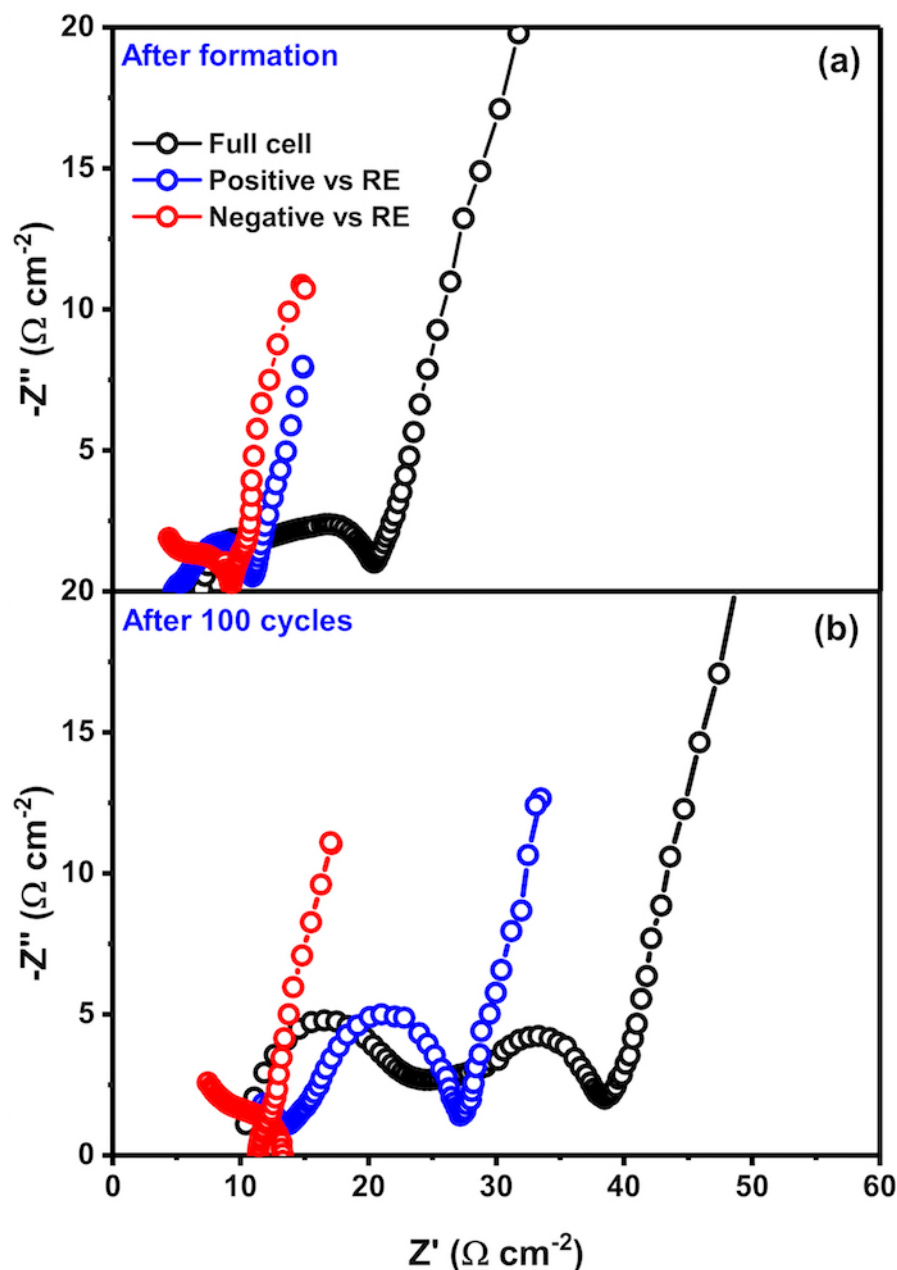


**Figure 3. Electrochemical Impedance Spectra of full cell, positive and negative electrodes**

AC- EIS spectra of all the full cell and the individual electrodes vs RE after (a) formation cycles and (b) 100 cycles. The EIS data is obtained by *in situ* lithiating Sn wire placed between the electrodes. Thus, a stable reference electrode can be used to gather impedance of individual electrode since unlike Li metal, the contribution to impedance from this thin wire is negligible providing accurate electrode behavior. [Please click here to view a larger version of this figure.](#)

## Discussion

**Figure 2a** is the voltage profile of the full cell while **Figure 2b** and **2c** show voltage profiles corresponding to the positive and the negative electrode vs  $\text{Li/Li}^+$  couple while the full cell is cycled between 3 and 4.4 V. It can be seen that as the full cell scans between 3 and 4.4 V, the positive electrode experiences voltages between 3.65 V and 4.45 V and the negative electrode between 0.65 V and 0.05 V vs.  $\text{Li/Li}^+$  respectively. During charge, the potential (vs.  $\text{Li/Li}^+$ ) of the positive increases indicating de-lithiation and that of the negative electrode (vs.  $\text{Li/Li}^+$ ) decreases indicating lithiation. In the first charge, as the potential of the negative electrode reaches  $\sim 1.1$  V, there is a change of slope and a small potential plateau. This is attributed to the reduction of FEC in the electrolyte<sup>18,19,20</sup>, forming an interfacial layer consuming Li-ions irreversibly. Decreased capacity during the subsequent discharge is shown as a voltage hysteresis in the profile. The hysteresis is reflected in the profile of the positive electrode and that of the full cell also. The potential profiles of individual electrodes are obtained as the Aux1 and Aux2 data from the Li metal reference electrode (step 3.2).



**Figure 3a** and **3b** represent the EIS of the full cell after formation cycles and at the end of the protocol collected using lithiated Sn wire as the RE as mentioned in step 3.3 (the measurements taken according to step 3.4). The 5 mV voltage amplitude during the EIS measurement does not activate electrochemical redox reactions and only the impedance response can be obtained. The frequency is varied between 10 mHz and 1 MHz. High frequency impedance provides information of the ohmic and interfacial behavior and mid- frequency impedance values indicate bulk response. The information about the diffusion coefficients of ions can be obtained from the low frequency region which appears as a straight line. Calculations relating to deconvolution of information from the spectra can be obtained from several literature articles<sup>21,22,23,24</sup>. It can be seen that there is a significant increase in the impedance of the full cell (black curve). The impedance data from individual positive and negative electrodes have also been plotted as blue and red curves respectively. While the negative electrode shows minor or no impedance rise, the increase in positive impedance is significant implying that the rise in full cell impedance predominantly comes from changes in positive impedance.

Electrochemical impedance of the couple involving Li metal are different from a pristine Li surface having a non-quantifiable contribution to the data. *In situ* lithiation of a secondary reference Cu/Sn wire forms metastable  $\text{Li}_x\text{Sn}$  alloys, whose chemical potentials are close to that of Li metal. The advantages of stable electrode potentials and being able to position the wire between the electrode sandwich facilitate this reliable design for obtaining impedance spectra of an electrode-reference couple. The efficacy of this reference electrode technique is understood when the impedance data of individual electrodes are plotted.

A major contribution to impedance of this couple comes from the electrode since no films are expected on the surface of the  $\text{Li}_x\text{Sn}$  wire. Precise monitoring of the impedance changes in the electrode can be facilitated through formation of *in situ* reference electrode. Since the  $\text{Li}_x\text{Sn}$  alloys are metastable, they undergo constant delithiation over time to obtain pure Sn electrode. However, the kinetics of self- discharge are extremely slow (> 200 hours for complete delithiation), facilitating nearly constant composition and potential throughout collection of the impedance spectra (time period ~ 0.5 hours for each electrode). This technique, thus, provides reliable EIS data compared to other techniques owing to the placement of the reference wire, the voltage of the  $\text{Li}_x\text{Sn}$  phase, etc. which render the data unaffected by ohmic losses and current density inhomogeneities. Despite great efficacy in the technique, the instability and low shelf life of the  $\text{Li}_x\text{Sn}$  wire due to self-discharge has been the only limitation since it requires re-lithiation of the Sn wire for measurements beyond 200 hours. Although the capacity lost in lithiating the Sn wire is low compared to the capacity of the cell, periodical re-lithiation over long term measurements may alter the state of charge of the positive electrode.

The approach can potentially be used to obtain *in situ* information about electrode behavior during the aging of a battery. Cycling a cell at extreme voltage conditions increase the chances of Li plating onto the negative electrode causing intense challenges of safety. Additional experiments are underway to understand the occurrence of Li plating by developing protocols to probe onset of Li deposition. Further, alloying Sn wire with other metals such as Na or Mg can widen the application of this technique to other new generation battery chemistries such as Na ion and Mg ion batteries.

## Disclosures

The authors have nothing to disclose.

## Acknowledgements

The authors acknowledge financial support from the U.S. Department of Energy, Office of Energy Efficiency and Renewable Energy.

## References

1. Delong, M., Zhanyi, C., & Anming, H. Si-Based Anode Materials for Li-ion Batteries: A Mini Review. *Nano-Micro Letters*. **6** (4) (2014).
2. Jung, S.-K. *et al.* Understanding the Degradation Mechanisms of  $\text{LiNi}_0.5\text{Co}_0.2\text{Mn}_0.3\text{O}_2$  Cathode Material in Lithium Ion Batteries. *Advanced Energy Materials*. **4** (1), 1300787-n/a (2014).
3. Streipert, B. *et al.* Influence of  $\text{LiPF}_6$  on the Aluminum Current Collector Dissolution in High Voltage Lithium Ion Batteries after Long-Term Charge/Discharge Experiments. *Journal of The Electrochemical Society*. **164** (7), A1474-A1479 (2017).
4. Gilbert, J. A. *et al.* Cycling Behavior of NCM523/Graphite Lithium-Ion Cells in the 3-4.4 V Range: Diagnostic Studies of Full Cells and Harvested Electrodes. *Journal of The Electrochemical Society*. **164** (1), A6054-A6065 (2017).
5. Shim, J., Kostecki, R., Richardson, T., Song, X., & Striebel, K. A. Electrochemical analysis for cycle performance and capacity fading of a lithium-ion battery cycled at elevated temperature. *Journal of Power Sources*. **112** (1), 222-230 (2002).
6. Peled, E., & Menkin, S. Review-SEI: Past, Present and Future. *Journal of The Electrochemical Society*. **164** (7), A1703-A1719 (2017).
7. Nadimpalli, S. P. V. *et al.* Quantifying capacity loss due to solid-electrolyte-interphase layer formation on silicon negative electrodes in lithium-ion batteries. *Journal of Power Sources*. **215**, 145-151 (2012).
8. Ender, M., Weber, A., & Ellen, I.-T. Analysis of Three-Electrode Setups for AC-Impedance Measurements on Lithium-Ion Cells by FEM simulations. *Journal of The Electrochemical Society*. **159** (2), A128-A136 (2011).
9. Zhou, J., & Notten, P. H. L. Development of Reliable Lithium Microreference Electrodes for Long-Term In Situ Studies of Lithium-Based Battery Systems. *Journal of The Electrochemical Society*. **151** (12), A2173-A2179 (2004).
10. Klink, S., Höche, D., La Mantia, F., & Schuhmann, W. FEM modelling of a coaxial three-electrode test cell for electrochemical impedance spectroscopy in lithium ion batteries. *Journal of Power Sources*. **240** (Supplement C), 273-280 (2013).
11. Bünzli, C., Kaiser, H., & Novák, P. Important Aspects for Reliable Electrochemical Impedance Spectroscopy Measurements of Li-Ion Battery Electrodes. *Journal of The Electrochemical Society*. **162** (1), A218-A222 (2015).
12. Delacourt, C., Ridgway, P. L., Srinivasan, V., & Battaglia, V. Measurements and Simulations of Electrochemical Impedance Spectroscopy of a Three-Electrode Coin Cell Design for Li-Ion Cell Testing. *Journal of The Electrochemical Society*. **161** (9), A1253-A1260 (2014).
13. Hoshi, Y. *et al.* Optimization of reference electrode position in a three-electrode cell for impedance measurements in lithium-ion rechargeable battery by finite element method. *Journal of Power Sources*. **288** (Supplement C), 168-175 (2015).

14. La Mantia, F., Wessells, C. D., Deshazer, H. D., & Cui, Y. Reliable reference electrodes for lithium-ion batteries. *Electrochemistry Communications*. **31** (Supplement C), 141-144 (2013).
15. Aurbach, D., Zinigrad, E., Cohen, Y., & Teller, H. A short review of failure mechanisms of lithium metal and lithiated graphite anodes in liquid electrolyte solutions. *Solid State Ionics*. **148** (3), 405-416 (2002).
16. Klett, M. *et al.* Electrode Behavior RE-Visited: Monitoring Potential Windows, Capacity Loss, and Impedance Changes in Li<sub>1.03</sub>(Ni<sub>0.5</sub>Co<sub>0.2</sub>Mn<sub>0.3</sub>)<sub>0.97</sub>O<sub>2</sub>/Silicon-Graphite Full Cells. *Journal of The Electrochemical Society*. **163** (6), A875-A887 (2016).
17. Zhang, W.-J. A review of the electrochemical performance of alloy anodes for lithium-ion batteries. *Journal of Power Sources*. **196** (1), 13-24 (2011).
18. Klett, M., Gilbert, J. A., Pupek, K. Z., Trask, S. E., & Abraham, D. P. Layered Oxide, Graphite and Silicon-Graphite Electrodes for Lithium-Ion Cells: Effect of Electrolyte Composition and Cycling Windows. *Journal of The Electrochemical Society*. **164** (1), A6095-A6102 (2017).
19. Ma, L. *et al.* A Guide to Ethylene Carbonate-Free Electrolyte Making for Li-Ion Cells. *Journal of The Electrochemical Society*. **164** (1), A5008-A5018 (2017).
20. Michan, A. L. *et al.* Fluoroethylene Carbonate and Vinylene Carbonate Reduction: Understanding Lithium-Ion Battery Electrolyte Additives and Solid Electrolyte Interphase Formation. *Chemistry of Materials*. **28** (22), 8149-8159 (2016).
21. Rahmoun, A., Loske, M., & Rosin, A. Determination of the Impedance of Lithium-ion Batteries Using Methods of Digital Signal Processing. *Energy Procedia*. **46**, 204-213 (2014).
22. Jiang, J. *et al.* Electrochemical Impedance Spectra for Lithium-ion Battery Ageing Considering the Rate of Discharge Ability. *Energy Procedia*. **105**, 844-849 (2017).
23. Andre, D. *et al.* Characterization of high-power lithium-ion batteries by electrochemical impedance spectroscopy. I. Experimental investigation. *Journal of Power Sources*. **196** (12), 5334-5341 (2011).
24. Li, S. E., Wang, B., Peng, H., & Hu, X. An electrochemistry-based impedance model for lithium-ion batteries. *Journal of Power Sources*. **258**, 9-18 (2014).